Solvent-Free Synthesis of Metal-Organic Frameworks Using Low-Melting Metal Salts

Tyler J. Azbell,[a] Tristan A. Pitt,[a] Melissa M. Bollmeyer,[a] Christina Cong,[a,†] Kyle M. Lancaster,[a] Phillip J. Milner[a,*]

[a]Department of Chemistry and Chemical Biology, Cornell University, Ithaca, NY 14850, United States

ABSTRACT: Metal-organic frameworks (MOFs) are porous, crystalline materials constructed from organic linkers and inorganic nodes with myriad potential applications in chemical separations, catalysis, drug delivery, and beyond. However, a major barrier to the application of MOFs in industry is their scalable synthesis, as most frameworks are prepared under highly dilute (≤0.01 M) solvothermal conditions using toxic organic solvents. Herein, we demonstrate that directly combining a range of salicylate and azolate linkers with low-melting metal halide (hydrate) salts above the melting point of the metal salt leads directly to high-quality MOFs without added solvent. Frameworks prepared under these ionothermal conditions possess high 77 K N_2 surface areas and crystallinities comparable to frameworks prepared under traditional solvothermal conditions, as confirmed by powder X-ray diffraction (PXRD) and scanning electron microscopy (SEM). In addition, we report the ionothermal syntheses of two frameworks that cannot be prepared directly under solvothermal conditions, namely, Fe_2X_2(dobdc) (dobdc^{4-} = 2,5-dioxido-1,4-benzenedicarboxylate) and Fe_2X_2(*m*-dobdc) (*m*-dobdc^{4-} = 4,6-dioxido-1,3-benzenedicarboxylate) (X = Cl, OH). These air-stable and porous Fe(III) members of the MOF-74 family possess pressed-pellet conductivities comparable to or higher than those of highly air-sensitive Fe(II) congeners. Overall, the simple solvent-free method reported herein should be broadly applicable to the discovery and sustainable synthesis of metal-organic materials.

INTRODUCTION

Metal–organic frameworks (MOFs) are porous, crystalline coordination polymers constructed from organic linkers and inorganic nodes that are promising next-generation materials for a range of applications, including chemical separations, gas storage, drug delivery, and heterogeneous catalysis.[1-4] (Semi)conducting MOFs are a unique class of materials with utility for electrochemical energy storage, electrocatalysis, and chemiresistive sensing.[5] Among MOFs, those constructed from basic linkers, including salicylates, pyrazolates, and triazolates, stand out due to their excellent chemical stabilities and highly modular structures.[6-10] However, the chemical stability of these MOFs is a double-edged sword, as poorly reversible metal-ligand bond formation generally necessitates harsh solvothermal reaction conditions to achieve high crystallinities. In particular, pyrazolate and triazolate MOFs are generally prepared under highly dilute reaction conditions (<0.01 M) in organic solvents such as *N*,*N*-dimethylformamide (DMF) due to the poor solubility of the corresponding organic linkers.[11-13] Techno-economic analyses confirm that organic solvents make up a large portion of the cost of MOFs on scale.[14] Therefore, scalable and sustainable methods for the synthesis of MOFs prepared from basic linkers would greatly accelerate their translation to industry.

Solvent-free methods are cost-effective and green alternatives to traditional, solvothermal (ST) methods.[15] Solvent-free MOF syntheses are generally carried out under mechanochemical conditions, in which solids are ground together with or without added liquid. Often, mechanical grinding results in MOFs with reduced crystallite sizes and porosities compared to their solvothermal congeners.[15-19] Mechanochemical methods also rely on specialized equipment such as ball mills, reducing their broad application. Ionothermal (IT) syntheses, in which an ionic liquid or molten metal salt is used as a solvent, structure directing agent, and/or reagent, are another promising alternative to traditional solvothermal methods using organic solvents.[20] In particular, a MOF synthesis in which a low-melting metal salt behaves as *both* the reaction solvent and metal precursor would minimize the waste associated with MOF preparation. However, it remains unclear if such an ionothermal strategy can be generalized beyond simple materials such as zeolitic imidazolate frameworks (ZIFs) and carboxylate MOFs.[16, 21-24] As such, ionothermal methods have significant untapped potential for the scalable, green, and time-efficient syntheses of stable MOFs.

Herein, we demonstrate that simply heating low-melting metal salt hydrates and organic linkers together above the melting point of the metal salt is a surprisingly general method for the synthesis of stable azolate and salicylate MOFs, especially those constructed from late first-row transition metals (Fe, Co, Ni, Zn). Nearly all of the frameworks prepared in this manner possess crystallinities and 77 K N_2 Brunauer–Emmett–Teller (BET) surface areas comparable to materials prepared under conventional, highly dilute solvothermal conditions. In addition, we demonstrate the first ionothermal synthesis of M(III) members of the MOF-74 family, which cannot be prepared directly under solvothermal conditions. Overall, our work demonstrates that the

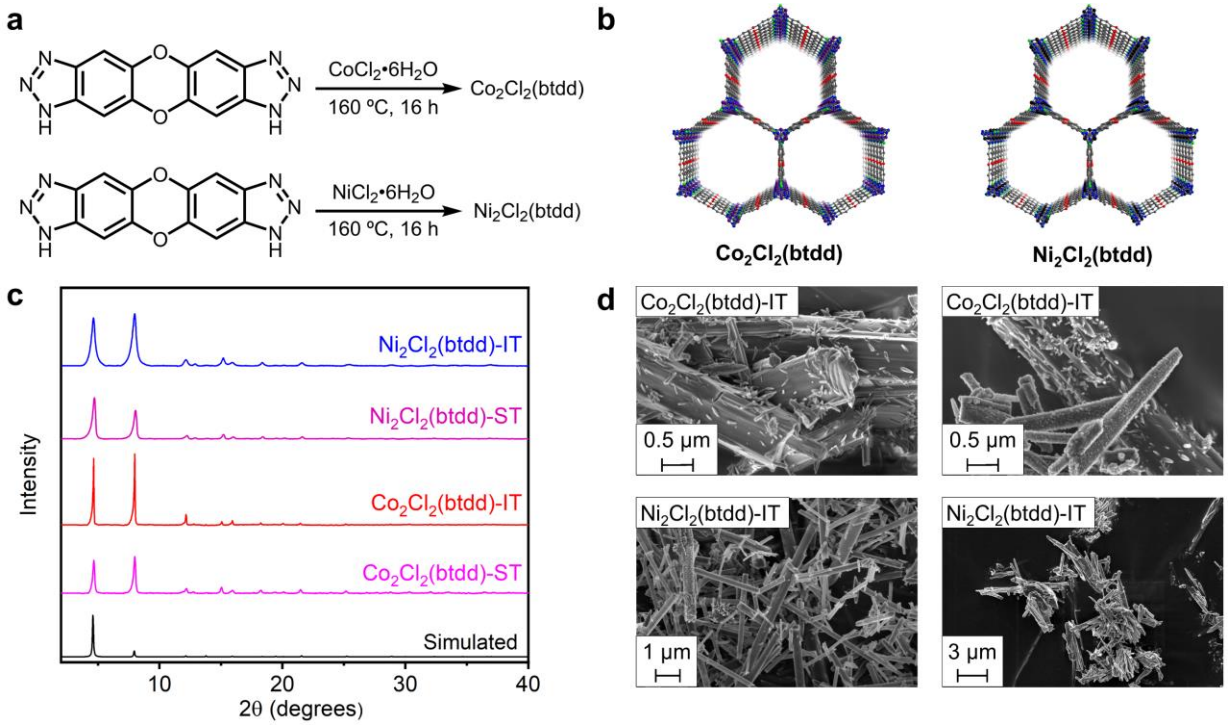

Figure 1. (a) Ionothermal synthesis of M_2Cl_2(btdd) (M = Co, Ni). (b) Structures of M_2Cl_2(btdd) (M = Co, Ni). Gray, white, red, green, blue, purple, and black spheres represent carbon, hydrogen, oxygen, chlorine, nitrogen, cobalt, and nickel, respectively. (c) PXRD patterns of M_2Cl_2(btdd) (M = Co, Ni) synthesized under solvothermal (ST) and ionothermal (IT) conditions. The experimental PXRD patterns were baseline corrected. (d) SEM images of M_2Cl_2(btdd) (M = Co, Ni) prepared under ionothermal conditions.

ionothermal synthesis of MOFs using low-melting metal salt hydrates as both the metal precursor and reaction medium represents a simple, scalable, and broadly applicable method for the synthesis of both known and new metal-organic materials.

RESULTS AND DISCUSSION

The proposed ionothermal synthesis of MOFs requires low-melting metal salts that can serve as both the MOF precursor and reaction medium. However, the high temperatures required for the application of most anhydrous metal salts (*e.g.*, $CoCl_2$, melting point = 735 °C) as solvents or templating agents would result in MOF decomposition (see, for example, SI Figure S16).[25] Intriguingly, metal salt hydrates (e.g. $CoCl_2{\cdot}6H_2O$, melting point = 86 °C) typically have much lower melting points than anhydrous metal salts, yet these reagents have not been previously studied as solvents for the ionothermal syntheses of porous materials.[25-29] Herein, ionothermal syntheses were performed using judiciously chosen low-melting metal salts in Teflon autoclaves (see Supporting Information or SI for details). The resulting frameworks were soaked in DMF and methanol to remove soluble impurities and then activated under dynamic vacuum prior to characterization. In all cases, the quality of prepared frameworks was assessed by powder X-ray diffraction (PXRD), infrared (IR) spectroscopy, scanning electron microscopy (SEM), and 77 K N_2 surface area analysis. The elemental purity of all samples was further validated qualitatively by X-ray photoelectron spectroscopy (XPS) and quantitatively by combustion analysis. All frameworks were prepared under both ionothermal and reported solvothermal conditions for direct comparison.

The M_2Cl_2(btdd) (M = V, Mn, Fe, Co, Ni, Cu; $btdd^{2-}$ = bis(1,2,3-triazolo[4,5-b],[4′,5′-i])dibenzo[1,4]dioxin) family of MOFs, which bear coordinatively unsaturated metal centers capable of strongly binding guest molecules, embody the synthetic challenges associated with preparing azolate MOFs (Figure 1a–b).[8, 11, 30-32] Due to the poor solubility of H_2btdd, these MOFs are generally prepared under highly dilute (0.001–0.005 M) solvothermal conditions and thus are routinely prepared on small scale in the laboratory. Improved methods for preparing Ni_2Cl_2(btdd) have been reported, but these syntheses still require dilute reactions conditions[30] and/or complex instrumentation.[33]

We began by investigating the ionothermal synthesis of Co_2Cl_2(btdd), also known as MAF-X27*l*-Cl,[34] as a representative member of this family of materials. Gratifyingly, simply heating stoichiometric amounts of $CoCl_2{\cdot}6H_2O$ and H_2btdd together in a Teflon autoclave at 160 °C yielded Co_2Cl_2(btdd) (referred to herein as Co_2Cl_2(btdd)-IT) without any crystalline impurities in good yield (66% on average), as confirmed by PXRD (Figure 1c, see SI Section 3 for details).[12] Notably, the crystallinity of the obtained MOF was comparable to that of material prepared under traditional solvothermal conditions at a linker concentration of ~0.002 M (Co_2Cl_2(btdd)-ST) (SI Figure S12). Analysis of Co_2Cl_2(btdd)-IT by SEM revealed that this material is composed of well-defined 2–5 μm rod-shaped crystals with additional smaller (<200 nm) crystallites (Figure 1d, SI Figure S22), consistent with the reported morphology of M_2Cl_2(btdd) MOFs.[35] In addition, the 77 K N_2 Brunauer-Emmett-Teller (BET) surface area of Co_2Cl_2(btdd) prepared under ionothermal conditions (2322 m^2/g, SI Figure S14) is nearly the same as that of MOF prepared under solvothermal conditions (2438 m^2/g, SI Figure S10) and higher than

that previously reported for this material (1912 m^2/g) (Table 1).[35] Combustion elemental analysis was also consistent with the predicted elemental composition for $Co_2Cl_2(btdd)$ (SI Table S2), confirming a lack of significant graphitization.[36, 37] Similar results were obtained for a second sample prepared under identical conditions (see SI Section 15 for details), supporting the reproducibility of the ionothermal synthesis of $Co_2Cl_2(btdd)$. Overall, these data confirm the high quality of $Co_2Cl_2(btdd)$-IT compared to material prepared under solvothermal conditions.

Table 1. 77 K N_2 Brunauer-Emmett-Teller (BET) surface areas of MOFs prepared under ionothermal and solvothermal conditions.

MOF	Ionothermal BET (m^2/g)	Solvothermal BET (Lit.) (m^2/g)
$Co_2Cl_2(btdd)$	2322	2438 (1912)[35]
$Ni_2Cl_2(btdd)$	2438	1973 (1763)[30]
$Zn_5Cl_4(btdd)_3$	2524	2750 (2750)[38]
$Ni_3(btp)_2$	2602	2100 (1650)[12]
Ni(bdp)	626	754 (1066) [39]
$Co_2(dobdc)$	1042	1135 (1382)[40]
$Fe_2X_2(dobdc)$	56	-
$Ni_2(m\text{-}dobdc)$	1416	1592 (1321) [41]
$Fe_2X_2(m\text{-}dobdc)$	402	-

Several control experiments were carried out to probe the pathway for $Co_2Cl_2(btdd)$ formation under ionothermal conditions (see SI Section 14 for details). As expected, an attempted ionothermal synthesis using anhydrous $CoCl_2$ at 160 °C yielded unreacted starting materials (SI Figure S138), confirming the need for waters of hydration to reduce the melting point of the metal salt precursor. We cannot rule out that water also serves a dual role as a supercritical solvent under these conditions. Heating H_2btdd and $CoCl_2{\cdot}6H_2O$ together at 90 °C— only 3 °C above the melting point of the metal salt—yielded an amorphous solid (SI Figure S139). Last, analysis of a crude ionothermal reaction mixture (*i.e.,* before washing with organic solvent to remove soluble impurities) by PXRD revealed that $Co_2Cl_2(btdd)$ is indeed the major crystalline product of the reaction (SI Figures S140–141). These findings indicate that melting $CoCl_2{\cdot}6H_2O$ and H_2btdd together well above the melting point of the metal salt produces $Co_2Cl_2(btdd)$ without added solvent.

To evaluate the scope of triazolate MOFs that can be prepared under ionothermal conditions, we extended our investigation to the isostructural Ni-analogue $Ni_2Cl_2(btdd)$ ($Ni_2Cl_2(btdd)$-IT, Figure 1a–b), also known as MAF-X28*l*-Cl,[34] and the polymorphic Zn-analogue $Zn_5Cl_4(btdd)_3$ ($Zn_5Cl_4(btdd)_3$-IT, Figure 2a–b), also known as MFU-4*l*.[38, 42] As with $Co_2Cl_2(btdd)$-IT, $Ni_2Cl_2(btdd)$-IT can be prepared directly from $NiCl_2{\cdot}6H_2O$ (melting point = 140 °C) and H_2btdd at 160 °C without added solvent (see SI Section 4 for details). The high crystallinity of $Ni_2Cl_2(btdd)$-IT was confirmed by PXRD and SEM (Figure 1c–d; SI Figures S23 and S37). Critically, $Ni_2Cl_2(btdd)$-IT possesses a 77 K N_2 BET surface area of 2438 m^2/g (SI Figure S28), comparable to the Co analogue but significantly higher than that measured for $Ni_2Cl_2(btdd)$ prepared under solvothermal conditions

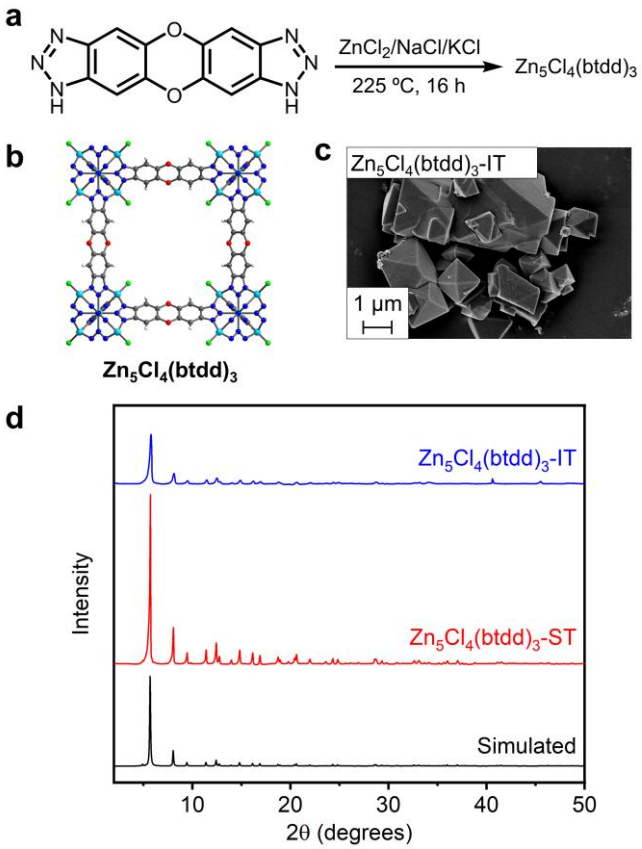

Figure 2. (a) Ionothermal synthesis of $Zn_5Cl_4(btdd)_3$. (b) Structure of $Zn_5Cl_4(btdd)_3$. (c) SEM image of $Zn_5Cl_4(btdd)_3$ prepared under ionothermal conditions. (d) PXRD patterns of $Zn_5Cl_4(btdd)_3$ synthesized under solvothermal (ST) and ionothermal (IT) conditions. The experimental PXRD patterns were baseline corrected.

(1973 m^2/g) (Table 1).[11] This represents one of the highest surface area reported to date for $Ni_2Cl_2(btdd)$, a promising MOF for water harvesting and corrosive gas capture.[11]

Given the high melting point of $ZnCl_2$ (290 °C), initial attempts to prepare $Zn_5Cl_4(btdd)_3$ directly from $ZnCl_2$ and H_2btdd resulted in partially degraded or graphitized material.[36, 37, 43, 44] In order to access high-quality samples of this framework, a 6:1:1 eutectic mixture of $ZnCl_2$, NaCl, and KCl with a melting point of 225 °C was employed as the reaction medium under anhydrous conditions instead.[45] The excess NaCl and KCl could be washed away by soaking the synthesized MOF in water. Ionothermal synthesis via this eutectic route afforded $Zn_5Cl_4(btdd)_3$-IT with a PXRD pattern matching that of the solvothermal analogue $Zn_5Cl_4(btdd)_3$-ST and the simulated pattern for this material (Figure 2d, see SI section 5 for details).[38] The SEM images of $Zn_5Cl_4(btdd)_3$-IT also reveal some well-defined octahedral crystals approximately 1–10 μm in length, in line with the expected morphology of this material, along with other less well-defined crystallites (Figure 2c, SI Figure S52).[38, 46, 47] In addition, 77 K N_2 adsorption measurements demonstrate that $Zn_5Cl_4(btdd)_3$-IT has a BET surface area of 2524 m^2/g (SI Figure S43), which is in good agreement with both the surface area of the solvothermal sample (2750 m^2/g) and values reported previously in the literature (2750 m^2/g) (Table 1).[38] While the obtained MOF was slightly gray in color, indicative of partial graphitization,[36] the carbon weight % of

$Zn_5Cl_4(btdd)_3$-IT measured by combustion analysis (34.21%) is in excellent agreement with the theoretical value (34.27%), suggesting that the degree of graphitization is likely minimal (SI Table S6). Because this synthesis was set up in a N_2-filled glovebox to minimize hydrolysis of $ZnCl_2$, we hypothesize that water is not necessary to form triazolate MOFs under solvent-free conditions, and that the molten salt itself directly facilitates MOF assembly in this case. Together, these results support that ionothermal methods can be generally employed to prepare Co, Ni, and Zn-based frameworks constructed from the $btdd^{2-}$ linker. Attempts to extend this ionothermal method to the synthesis of less robust Mn- and Cu-based analogues were unsuccessful,[7, 11, 48] suggesting that ionothermal methods are best suited for the synthesis of thermodynamically stable azolate frameworks constructed from strong M–N bonds.

Encouraged by the successful synthesis of several triazolate frameworks under ionothermal conditions, we next investigated the generality of this strategy towards the synthesis of frameworks constructed from more basic pyrazolate linkers. One such framework of interest is $Ni_3(btp)_2$ (btp^{3-} = 4,4',4''-(benzene-1,3,5-triyl)tris(pyrazolate)), which is a thermally and chemically robust MOF bearing coordinatively unsaturated square planar Ni(II) centers in an overall sodalite topology (Figure 3).[12] The unsaturated metal centers of $Ni_3(btp)_2$ make it a promising heterogeneous catalyst for the solvent-free cycloaddition of CO_2 and epoxides to form cyclic carbonates.[49] The traditional solvothermal synthesis of $Ni_3(btp)_2$ employs $Ni(OAc)_2{\cdot}4H_2O$ as the metal precursor and is carried out in dilute DMF (0.05 M).[12] Switching from $Ni(OAc)_2{\cdot}4H_2O$, which decomposes upon heating, to $NiCl_2{\cdot}6H_2O$ as the metal precursor and reaction medium enabled the ionothermal synthesis of $Ni_3(btp)_2$-IT under the same conditions employed to prepare $Ni_2Cl_2(btdd)$-IT (Figure 3, see SI section 6 for details). The crystallinity of $Ni_3(btp)_2$-IT was found to be superior to material prepared under the traditional solvothermal conditions by PXRD ($Ni_3(btp)_2$-ST, Figure 3d). Likewise, the BET surface area of $Ni_3(btp)_2$-IT (2602 m^2/g, SI Figure S58) is significantly higher than that of $Ni_3(btp)_2$-ST (2100 m^2/g) (Table 1).[12] This may be due in part to the presence of missing linker and/or node defects in $Ni_3(btp)_2$-IT, as evidenced by the presence of trace Cl in this sample by XPS even after soaking in DMF and methanol (SI Figure S61).[50-52] Together with the excellent results obtained for the synthesis of $Ni_2Cl_2(btdd)$-IT, these findings suggest that ionothermal methods are promising alternatives to solvothermal methods for the synthesis of high surface area Ni-azolate MOFs.

Our efforts to further extend these findings to the synthesis of the flexible Ni-pyrazolate MOF Ni(bdp)[39] (bdp^{2-} = 1,4-benzene-4,4′-dipyrazolate) under ionothermal conditions were moderately successful (see SI section 7 for details). While an insoluble, porous yellow solid (Ni(bdp)-IT) could be obtained by simply combining H_2bdp and $NiCl_2{\cdot}6H_2O$ at 160 °C, the PXRD of the resulting crystalline solid was slightly inconsistent with that previously reported for Ni(bdp)-ST prepared under solvothermal conditions (SI Figure S69). The most probable solution determined by Pawley refinements corresponds to a space group of Ima2 (indistinguishable from Imma, the reported space group of Ni(bdp)[39]) with a = 26.71 Å, b = 13.89 Å, c = 6.302 Å, α = 90

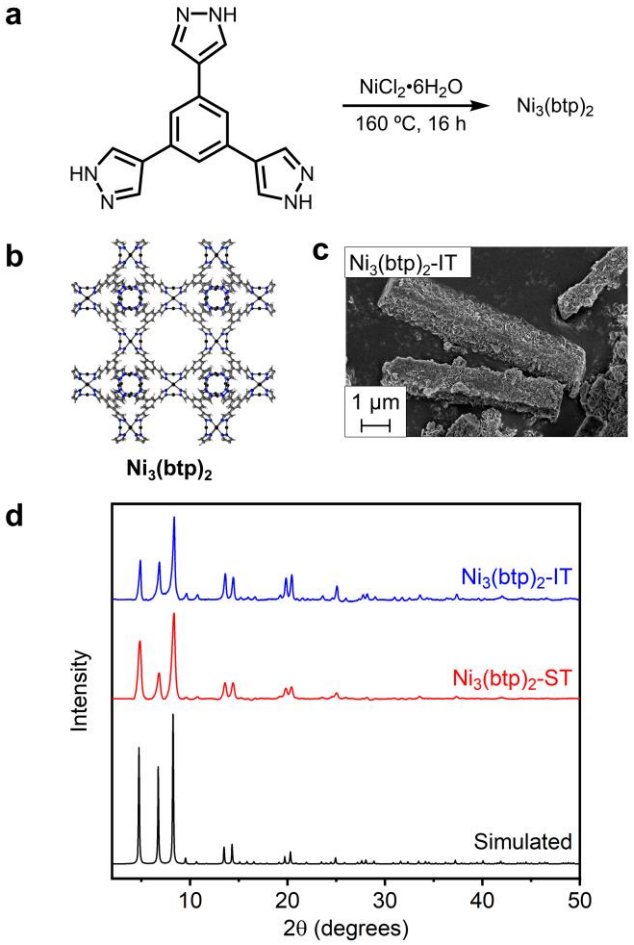

Figure 3. (a) Ionothermal synthesis of $Ni_3(btp)_2$. (b) Structure of $Ni_3(btp)_2$. Gray, white, blue, and black spheres correspond to carbon, hydrogen, nitrogen, and nickel, respectively. (c) SEM image of $Ni_3(btp)_2$ prepared under ionothermal conditions. (d) PXRD patterns of $Ni_3(btp)_2$ synthesized under solvothermal (ST) and ionothermal (IT) conditions. The experimental PXRD patterns were baseline corrected.

° (SI Figure S70), which is significantly expanded in a compared to the previously reported structure of Ni(bdp)-ST (a = 22.7353(32), Å, b = 13.4648(14) Å, c = 6.76552(46) Å, α = 90 °). Given the reported flexibility of this framework,[39] we hypothesize that Ni(bdp)-IT is likely a slightly different but related phase of this material. Consistently, the BET surface area of activated Ni(bdp)-IT (626 m^2/g) is lower than that reported for Ni(bdp) (1066 m^2/g) (Table 1). This finding underlines the intriguing possibility of employing ionothermal methods to prepare alternative phases of flexible MOFs.

Given the generality of this ionothermal strategy for the synthesis of MOFs constructed from basic pyrazolate and triazolate linkers, we aimed to expand our findings to MOFs constructed from another class of basic linkers: salicylates. Among salicylate MOFs, $M_2(dobdc)$ ($dobdc^{4-}$ = 2,5-dioxido-1,4-benzenedicarboxylate), also known as MOF-74 or CPO-27, and $M_2(m\text{-}dobdc)$ (m-$dobdc^{4-}$ = 4,6-dioxido-1,3-benzenedicarboxylate), stand out due to their high density of coordinatively unsaturated M(II) sites (Figures 4a–b).[39, 40] Although mechanochemical methods to synthesize these frameworks have been previously reported, they typically produce materials with modest crystallinities and reduced porosities compared to traditional solvothermal methods.[19]

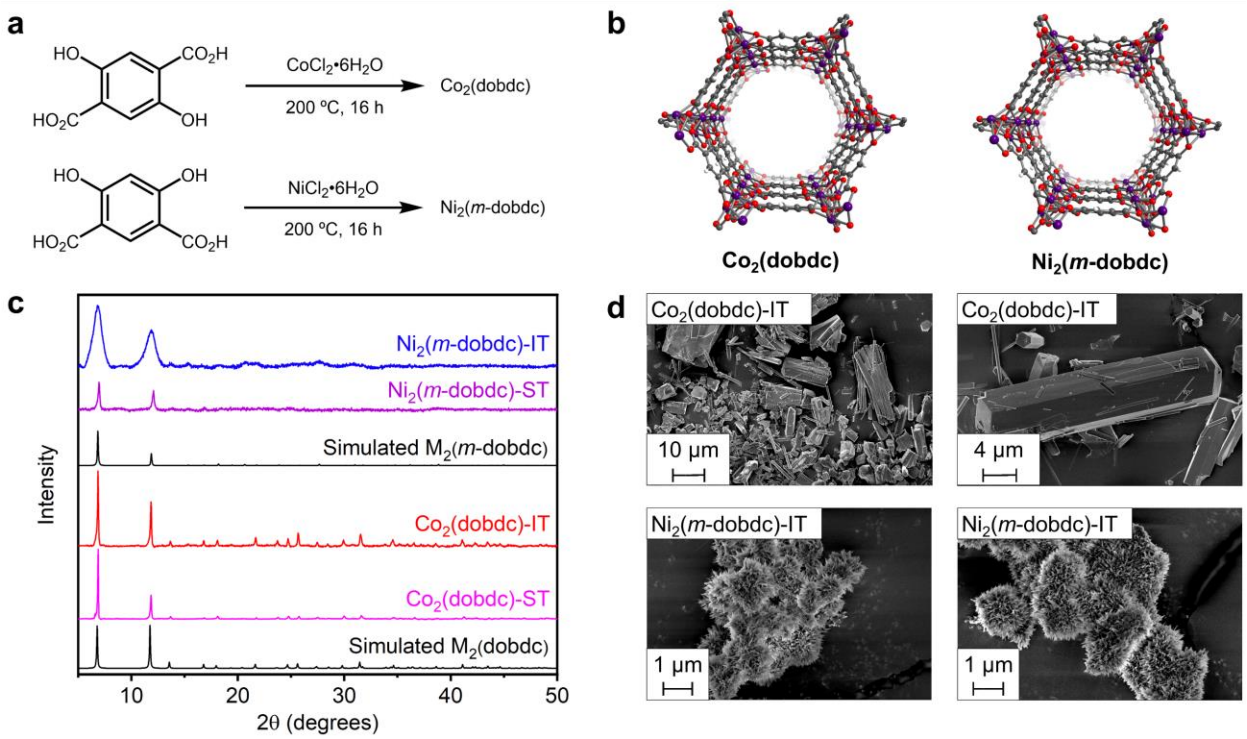

Figure 4. (a) Ionothermal synthesis of Co_2(dobdc) and Ni_2(*m*-dobdc). (b) Structures of Co_2(dobdc) and Ni_2(*m*-dobdc). Gray, white, red, purple, and black spheres correspond to carbon, hydrogen, oxygen, cobalt, and nickel, respectively. (c) PXRD patterns of Co_2(dobdc) and Ni_2(*m*-dobdc) synthesized under solvothermal (ST) and ionothermal (IT) conditions. The experimental PXRD patterns were baseline corrected. (d) SEM images of Co_2(dobdc) and Ni_2(*m*-dobdc) prepared under ionothermal conditions.

As such, ionothermal methods represent a promising alternative to synthesize salicylate MOFs constructed from late transition metals under solvent-free conditions. Of primary interest are Co_2(dobdc), which is a promising material for separating xylene isomers,[53] and Ni_2(*m*-dobdc) (*m*-dobdc^{4-} = 4,6-dioxido-1,3-benzenedicarboxylate), a record-holding material for H_2 storage that we recently demonstrated is one of the most chemically stable salicylate MOFs as well (Figure 4).[6, 54] Both of these frameworks are typically synthesized under dilute solvothermal conditions (0.01–0.05 M)[41, 55] using mixtures of DMF and alcohol solvents. Therefore, we investigate whether the ionothermal conditions employed to prepare Co_2Cl_2(btdd) and Ni_2Cl_2(btdd) were generalizable to the synthesis of Co_2(dobdc) and Ni_2(*m*-dobdc) (see SI Sections 8 and 10 for details).

Initial attempts to synthesize Co_2(dobdc) and Ni_2(*m*-dobdc) directly from $CoCl_2{\cdot}6H_2O$ and $NiCl_2{\cdot}6H_2O$, respectively, under ionothermal conditions at 160 °C were unsuccessful (not shown). However, simply increasing the reaction temperature to 200 °C was sufficient to enable the synthesis of phase-pure Co_2(dobdc)-IT and Ni_2(*m*-dobdc)-IT, as confirmed by PXRD (Figure 4c). The crystallinity of Co_2(dobdc)-IT was comparable to that of material prepared under solvothermal conditions, while the crystallinity of Ni_2(*m*-dobdc)-IT was more modest. These findings were confirmed by SEM, as Co_2(dobdc)-IT is composed of well-defined crystallites, including some hexagonal rods >10 μm in length (Figure 4d, SI Figure S92). On the other hand, Ni_2(*m*-dobdc)-IT consists of fuzzy microcrystalline particles (Figure 4d, SI Figure S119). As with the azolate MOFs discussed above, the 77 K N_2 BET surface areas of Co_2(dobdc)-IT and Ni_2(*m*-dobdc)-IT are comparable to those of reference materials prepared under solvothermal conditions and to values reported in the literature (Table 1), reflecting their high quality.[40, 56] Consistently, neither material was found to contain significant amounts of residual Cl, as confirmed by XPS (SI Figures S88, S115). These promising results suggest that ionothermal methods may be a general alternative to solvothermal methods for the synthesis of stable Co- and Ni-based MOFs constructed from basic linkers.

Having demonstrated the surprising generality of ionothermal methods for the synthesis of azolate and salicylate MOFs, we hypothesized that the unusual kinetic regime offered by ionothermal methods might enable the synthesis of new frameworks that cannot be synthesized directly under solvothermal conditions. To investigate this possibility, we targeted the synthesis of M(III) variants of the M_2(dobdc) and M_2(*m*-dobdc) families of materials. Although both frameworks can be prepared with a range of M(II) cations (*e.g.,* Mg, Mn, Fe, Co, Ni, Cu, Zn, Cd),[57] the direct synthesis of M(III) variants of these frameworks remains unreported. Consistently, attempted direct syntheses of Fe_2Cl_2(dobdc) and Fe_2Cl_2(*m*-dobdc) from $FeCl_3{\cdot}6H_2O$ and the corresponding linkers under the solvothermal conditions typically used to prepare Fe_2(dobdc) and Fe_2(*m*-dobdc) produced only amorphous solids (SI Figures S106 and S134). Previously reported Fe(III) variants of MOF-74 have been prepared via post-synthetic oxidation of highly air-sensitive Fe_2(dobdc) with limited success.[58-62] Therefore, we investigated

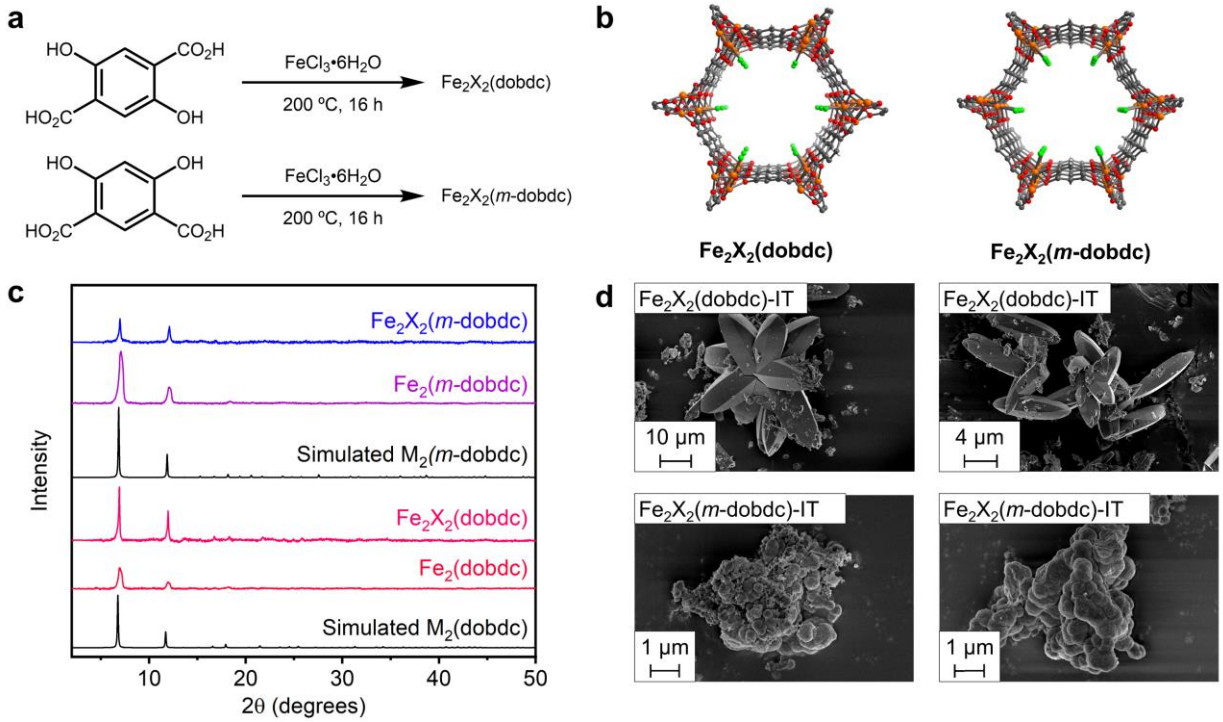

Figure 5. (a) Ionothermal synthesis of Fe_2X_2(dobdc) and Fe_2X_2(*m*-dobdc) (X = Cl, OH). (b) Structures of Fe_2X_2(dobdc) and Fe_2X_2(*m*-dobdc) (X = Cl, OH). Gray, white, red, orange, and green spheres correspond to carbon, hydrogen, oxygen, iron, and chlorine, respectively. (c) PXRD patterns of Fe_2X_2(dobdc) and Fe_2X_2(*m*-dobdc) (X = Cl, OH) synthesized under solvothermal (ST) and ionothermal (IT) conditions. The experimental PXRD patterns were baseline corrected. (d) SEM images of Fe_2X_2(dobdc) and Fe_2X_2(*m*-dobdc) (X = Cl, OH) prepared under ionothermal conditions.

whether these understudied Fe(III) frameworks can be prepared directly under ionothermal conditions instead (see Sections 9 and 11 of the SI for details).

Initial attempts to prepare Fe(III) salicylate MOFs from $FeCl_3 \cdot 6H_2O$ and H_4dobdc or H_4*m*-dobdc under ionothermal conditions at 160–180 °C were unsuccessful (not shown). Increasing the reaction temperature to 200 °C—the same temperature employed to prepare Co_2(dobdc)-IT and Ni_2(*m*-dobdc)-IT—produced crystalline solids with PXRD patterns similar to those of independently prepared samples of Fe_2(dobdc) and Fe_2(*m*-dobdc), respectively (Figure 5c).[40, 56] This is not surprising, as these frameworks would be expected to adopt similar topologies as the corresponding Fe(II) frameworks with additional charge-balancing anions in the pores to compensate for the increase in metal formal oxidation state (Figure 5b).[41] The obtained air-stable solids were initially assigned as Fe_2X_2(dobdc) and Fe_2X_2(*m*-dobdc) (X = Cl, OH) due to uncertainty regarding the charge-balancing anions present in the framework pores (see discussion below).

Consistent with the PXRD data, SEM images of Fe_2X_2(dobdc) (X = Cl, OH) revealed clusters of ellipsoidal crystallites that range in size from 5–20 μm in length, akin to the SEM images of many MOF-74 analogues,[40, 63, 64] along with less well-defined particles (Figure 5d, SI Figure S104). In contrast, the SEM images of Fe_2X_2(*m*-dobdc) (X = Cl, OH) revealed poorly defined particles (Figure 5d, SI Figure S131), in line with the reduced crystallinity of this material. Further supporting the assigned structures, the 77 K N_2 BET surface areas of Fe_2X_2(dobdc) (X = Cl, OH) (56 m^2/g) and Fe_2X_2(*m*-dobdc) (X = Cl, OH) (402 m^2/g) (Table 1) are significantly lower than those reported for Fe_2(dobdc) (1350 m^2/g)[65] and Fe_2(*m*-dobdc) (1360 m^2/g),[41] respectively. This is expected, as the additional species within the pores of the Fe(III) MOFs should reduce their free pore volumes. The surface area of Fe_2X_2(*m*-dobdc) is likely also reduced due to partial graphitization under the ionothermal conditions (SI Table S18).[36] In contrast, the %C determined by combustion analysis of Fe_2X_2(dobdc) (X = Cl, OH) (29.96%) is comparable to the theoretical value (25.51–28.28%), suggesting that minimal graphitization of this material occured under the reaction conditions (SI Table S13).

We employed Mössbauer spectroscopy to further support the formal oxidation state assignments of the novel Fe(III) MOFs (Figure 6). The Mössbauer spectrum of Fe_2X_2(dobdc) (X = Cl, OH) contains a doublet corresponding to a single Fe species with an isomer shift of 0.51 mm/s and a quadrupole splitting of 0.90 mm/s, consistent with an S = 5/2 Fe(III) species (SI Table S14). Likewise, Fe_2X_2(*m*-dobdc) (X = Cl, OH) possess a similar Mössbauer spectrum with an isomer shift of 0.50 mm/s and a quadrupole splitting of 0.88 mm/s, again consistent with an S = 5/2 Fe(III) center (SI Table S19). These values are comparable to those previously reported for Fe(III) MOF-74 prepared by post-synthetic oxidation.[59] The Mössbauer spectra of the Fe(III) MOFs contrast with that of a reference sample of Fe_2(dobdc), which contains a doublet with an increased isomer shift of 1.26(6) mm/s and a quadrupole splitting of 2.58 mm/s (Figure 6, SI Table S21). These parameters are consistent with a $S = 2$ Fe(II) center and are similar to reported values for this framework as well.[60, 62] Overall, the PXRD, SEM, 77 K N_2 BET surface areas, and Mössbauer spectra are consistent with the structural assignment of Fe_2X_2(dobdc) and Fe_2X_2(*m*-

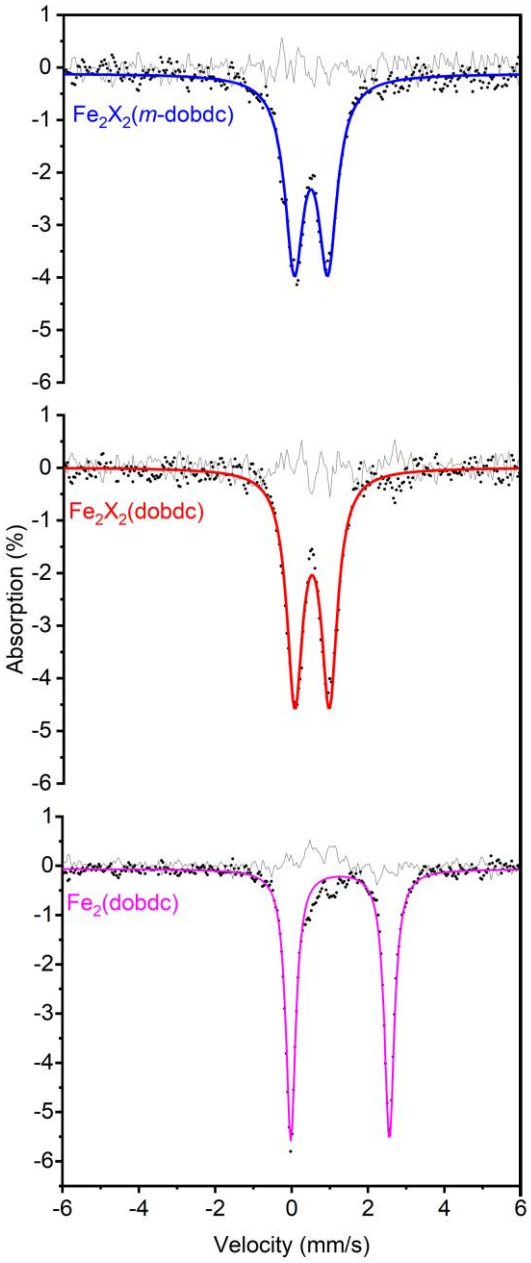

Figure 6. Mössbauer profiles of the Fe(III) MOFs Fe_2X_2(*m*-dobdc) and Fe_2X_2(dobdc) (X = Cl, OH). The Mössbauer profile of the Fe(II) MOF Fe_2(dobdc) is included for comparison.

dobdc) (X = Cl, OH) as Fe(III) analogues of M_2(dobdc) and M_2(*m*-dobdc) MOFs, respectively.[58, 59, 66, 67]

After establishing the likely structures of the new Fe(III) frameworks, we investigated the nature of the charge-balancing anions—Cl, OH, or a mixture of both—present within the pores. Combustion analysis of both materials revealed that the Cl wt% was low for both materials assuming molecular formulae of Fe_2Cl_2(dobdc) (Table S13) and Fe_2Cl_2(*m*-dobdc) (Table S18), respectively. In addition, the XPS spectra of both materials, while not quantitative,[68] revealed weaker-than-expected signals for Cl in the high-resolution spectra (Figures S98 and S125). Last, energy-dispersive X-ray spectroscopy (EDS) of both materials revealed relatively uniform distributions of Fe and O species among particles, but more sparse Cl occupancies on the particle surfaces (SI Figures S105 and S132). Together, these results indicate that the charge-balancing anions are likely a mixture of Cl^- and OH^- in both Fe_2X_2(dobdc) and Fe_2X_2(*m*-dobdc) (X = Cl, OH). The disordered nature of the charge-balancing anions within the pores of both materials likely contributes to their reduced 77 K N_2 BET surface areas compared to the Fe(II) congeners.

It is well-known that MOFs containing Fe-based secondary building units demonstrate higher electrical conductivities compared to frameworks constructed from other first row transition metals.[69, 70] Indeed, Fe_2(dobdc) possesses a pressed pellet conductivity more than six orders of magnitude higher than other M_2(dobdc) analogues.[69] Notably, Fe_2X_2(dobdc) and Fe_2X_2(*m*-dobdc) (X = Cl, OH) were found to possess pressed-pellet conductivities on the order of 10^{-7} S/cm (SI Table S20), approximately one order of magnitude higher than the electrical conductivity reported for Fe_2(dobdc).[70] In particular, Fe_2X_2(dobdc) (X = Cl, OH) demonstrates a pressed-pellet conductivity of 6.6×10^{-7} S/cm, which is similar to the reported value of 5.8×10^{-7} S/cm for Fe_2(dsbdc) ($dsbdc^{4-}$ = 2,5-sulfidobenzene-1,4-dicarboxylate), the previously reported record pressed-pellet conductivity for a MOF-74 analogue.[69] In addition, compared to the known Fe(II) MOFs, the Fe(III) MOFs reported herein offer a significant improvement in their air and moisture stability, as both can be synthesized and washed in air while retaining their crystallinity.[60, 67] Overall, the successful syntheses of Fe_2X_2(*m*-dobdc) and Fe_2X_2(dobdc) (X = Cl, OH) under ionothermal but not solvothermal conditions demonstrate that ionothermal methods can provide access to robust MOFs with improved properties.

CONCLUSION

Ionothermal synthesis of MOFs offers a scalable, green alternative to traditional syntheses under dilute solvothermal conditions. In addition, the simple ionothermal conditions reported herein eschew the need for complex instrumentation and strenuous mechanochemical conditions that often lead to poorly crystalline materials. This unique approach to ionothermal synthesis involves the metal (hydrate) salt playing two roles: as the MOF precursor and as the reaction solvent. Employing this ionothermal method, we report the synthesis of seven known azolate and salicylate MOFs with high crystallinities and BET surface areas comparable to materials synthesized under traditional conditions. Additionally, we report the synthesis and pressed-pellet conductivities of two new M(III) salicylate MOFs. These frameworks represent the first directly synthesized Fe(III) MOF-74 analogues and possess improved air stabilities compared to their Fe(II) analogues. Our intriguing preliminary findings with Ni(bdp)-IT suggest that ionothermal methods may also be useful for accessing alternative phases of flexible MOFs as well. Future work will focus on strategies to reduce ionothermal synthesis temperatures to minimize graphitization and on the design of new low-melting metal precursors to further generalize this strategy to the preparation of other metal-organic materials.

ASSOCIATED CONTENT

Supporting Information. All synthetic procedures and characterization data. This material is available free of charge via the Internet at http://pubs.acs.org.

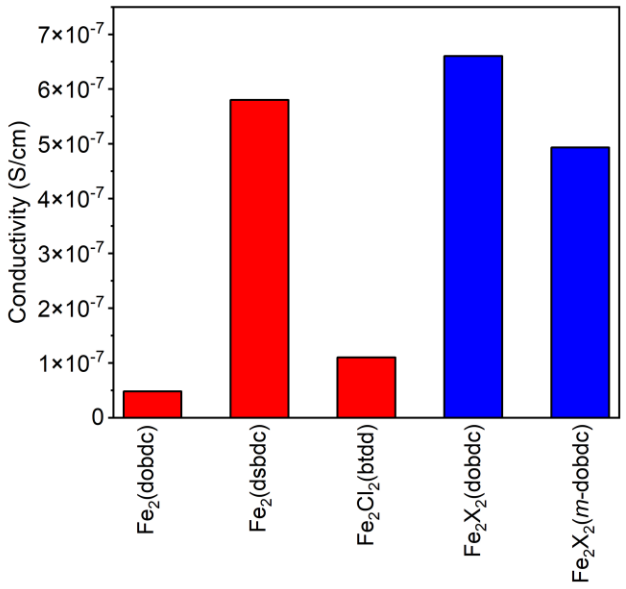

Figure 7. Pressed-pellet conductivities of known Fe(II) MOFs (red)[67] and Fe(III) MOFs synthesized under ionothermal conditions (blue).

AUTHOR INFORMATION

Corresponding Author

* pjm347@cornell.edu

Present Addresses

†Department of Chemistry, Princeton, NJ 08544, United States

Author Contributions

P.J.M. conceived the project. T.J.A. synthesized and characterized all MOF samples. T.A.P. collected SEM images. M.B.B. carried out all Mössbauer measurements and interpreted the results with K.M.L. C.C. synthesized all organic linkers. The manuscript was written through the contributions of all authors and all authors approved of the final version.

Funding Sources

The development of methods for the scalable synthesis of MOFs was supported by the National Institute of General Medical Sciences of the National Institutes of Health under award number R35GM138165 (T.J.A., T.A.P., C.C., P.J.M.). The content is solely the responsibility of the authors and does not necessarily represent the official views of the National Institutes of Health. T.J.A. thanks Cornell University for financial support through a recruiting fellowship. M.B.B. is an NSF Graduate Research Fellow. K.M.L. acknowledges NSF for support (CHE-1954515). We are grateful to Cornell University for providing a Summer Experience Grant to C.C. This work made use of the Cornell Center for Materials Research Shared Facilities, which are supported through the NSF MRSEC program (DMR-1719875). ^{1}H NMR data were collected on a Bruker INOVA 500 MHz spectrometer that was purchased with support from the National Science Foundation (CHE-1531632).

Notes

P.J.M. is listed as a co-inventor on several patents related to MOFs.

ACKNOWLEDGMENT

We thank Cara Gannett (Cornell University) for assistance with pressed pellet conductivity measurements. We are grateful to Ruth Mandel and Jaehwan Kim (Cornell University) for editorial assistance during the preparation of this manuscript. We thank Mary Zick (Cornell University) for the synthesis of Fe_2(dobdc).

REFERENCES

1. Li, H.; Li, L.; Lin, R.-B.; Zhou, W.; Zhang, Z.; Xiang, S.; Chen, B., Porous metal-organic frameworks for gas storage and separation: Status and challenges. *EnergyChem* **2019,** *1* (1), 100006.
2. Wang, C.; An, B.; Lin, W., Metal–Organic Frameworks in Solid–Gas Phase Catalysis. *ACS Catalysis* **2019,** *9* (1), 130-146.
3. Dhakshinamoorthy, A.; Li, Z.; Garcia, H., Catalysis and photocatalysis by metal organic frameworks. *Chem. Soc. Rev.* **2018,** *47* (22), 8134-8172.
4. Furukawa, H.; Cordova Kyle, E.; O'Keeffe, M.; Yaghi Omar, M., The Chemistry and Applications of Metal-Organic Frameworks. *Science* **2013,** *341* (6149), 1230444.
5. Xie, L. S.; Skorupskii, G.; Dincă, M., Electrically Conductive Metal–Organic Frameworks. *Chem. Rev.* **2020,** *120* (16), 8536-8580.
6. Wang, Z.; Bilegsaikhan, A.; Jerozal, R. T.; Pitt, T. A.; Milner, P. J., Evaluating the Robustness of Metal–Organic Frameworks for Synthetic Chemistry. *ACS Appl. Mater. Interfaces* **2021,** *13* (15), 17517-17531.
7. Feng, L.; Wang, K.-Y.; Day, G. S.; Ryder, M. R.; Zhou, H.-C., Destruction of Metal–Organic Frameworks: Positive and Negative Aspects of Stability and Lability. *Chem. Rev.* **2020,** *120* (23), 13087-13133.
8. Rieth, A. J.; Wright, A. M.; Dincă, M., Kinetic stability of metal–organic frameworks for corrosive and coordinating gas capture. *Nat. Rev. Mater.* **2019,** *4* (11), 708-725.
9. Yuan, S.; Feng, L.; Wang, K.; Pang, J.; Bosch, M.; Lollar, C.; Sun, Y.; Qin, J.; Yang, X.; Zhang, P.; Wang, Q.; Zou, L.; Zhang, Y.; Zhang, L.; Fang, Y.; Li, J.; Zhou, H.-C., Stable Metal–Organic Frameworks: Design, Synthesis, and Applications. *Adv. Mater.* **2018,** *30* (37), 1704303.
10. Liao, P.-Q.; He, C.-T.; Zhou, D.-D.; Zhang, J.-P.; Chen, X.-M., Porous Metal Azolate Frameworks. In The Chemistry of Metal-Organic Frameworks: Synthesis, Characterization, and Applications; Kaskel S, Ed.; Wiley-VCH Verlag GmbH & Co. KGaA: Weinheim, Germany, 2016; pp 309–343.
11. Rieth, A. J.; Tulchinsky, Y.; Dincă, M., High and Reversible Ammonia Uptake in Mesoporous Azolate Metal–Organic Frameworks with Open Mn, Co, and Ni Sites. *J. Am. Chem. Soc.* **2016,** *138* (30), 9401-9404.
12. Colombo, V.; Galli, S.; Choi, H. J.; Han, G. D.; Maspero, A.; Palmisano, G.; Masciocchi, N.; Long, J. R., High thermal and chemical stability in pyrazolate-bridged metal–organic frameworks with exposed metal sites. *Chem. Sci.* **2011,** *2* (7), 1311-1319.
13. Alder, C. M.; Hayler, J. D.; Henderson, R. K.; Redman, A. M.; Shukla, L.; Shuster, L. E.; Sneddon, H. F., Updating and further expanding GSK's solvent sustainability guide. *Green Chem.* **2016,** *18* (13), 3879-3890.
14. DeSantis, D.; Mason, J. A.; James, B. D.; Houchins, C.; Long, J. R.; Veenstra, M., Techno-economic Analysis of Metal–Organic Frameworks for Hydrogen and Natural Gas Storage. *Energy & Fuels* **2017,** *31* (2), 2024-2032.
15. Chen, D.; Zhao, J.; Zhang, P.; Dai, S., Mechanochemical synthesis of metal–organic frameworks. *Polyhedron* **2019,** *162*, 59-64.

16. Užarević, K.; Wang, T. C.; Moon, S.-Y.; Fidelli, A. M.; Hupp, J. T.; Farha, O. K.; Friščić, T., Mechanochemical and solvent-free assembly of zirconium-based metal–organic frameworks. *Chem. Commun.* **2016,** *52* (10), 2133-2136.
17. Klimakow, M.; Klobes, P.; Thünemann, A. F.; Rademann, K.; Emmerling, F., Mechanochemical Synthesis of Metal–Organic Frameworks: A Fast and Facile Approach toward Quantitative Yields and High Specific Surface Areas. *Chem. Mater.* **2010,** *22* (18), 5216-5221.
18. Friščić, T., Metal-Organic Frameworks: Mechanochemical Synthesis Strategies. *Encyclopedia of Inorganic and Bioinorganic Chemistry* **2014**, 1-19.
19. Wang, Z.; Li, Z.; Ng, M.; Milner, P. J., Rapid mechanochemical synthesis of metal–organic frameworks using exogenous organic base. *Dalton Trans.* **2020,** *49* (45), 16238-16244.
20. Parnham, E. R.; Morris, R. E., Ionothermal Synthesis of Zeolites, Metal–Organic Frameworks, and Inorganic–Organic Hybrids. *Acc. Chem. Res.* **2007,** *40* (10), 1005-1013.
21. Mao, Y.; Qi, H.; Ye, G.; Han, L.; Zhou, W.; Xu, W.; Sun, Y., Green and time-saving synthesis of MIL-100(Cr) and its catalytic performance. *Microporous Mesoporous Mater.* **2019,** *274*, 70-75.
22. Lestari, W. W.; Arvinawati, M.; Martien, R.; Kusumaningsih, T., Green and facile synthesis of MOF and nano MOF containing zinc(II) and benzen 1,3,5-tri carboxylate and its study in ibuprofen slow-release. *Mater. Chem. Phys.* **2018,** *204*, 141-146.
23. Leng, K.; Sun, Y.; Li, X.; Sun, S.; Xu, W., Rapid Synthesis of Metal–Organic Frameworks MIL-101(Cr) Without the Addition of Solvent and Hydrofluoric Acid. *Cryst. Growth Des.* **2016,** *16* (3), 1168-1171.
24. Gökpinar, S.; Diment, T.; Janiak, C., Environmentally benign dry-gel conversions of Zr-based UiO metal–organic frameworks with high yield and the possibility of solvent re-use. *Dalton Trans.* **2017,** *46* (30), 9895-9900.
25. Kuhn, P.; Forget, A.; Su, D.; Thomas, A.; Antonietti, M., From Microporous Regular Frameworks to Mesoporous Materials with Ultrahigh Surface Area: Dynamic Reorganization of Porous Polymer Networks. *J. Am. Chem. Soc.* **2008,** *130* (40), 13333-13337.
26. Kim, J.; Moisanu, C. M.; Gannett, C. N.; Halder, A.; Fuentes-Rivera, J. J.; Majer, S. H.; Lancaster, K. M.; Forse, A. C.; Abruña, H. D.; Milner, P. J., Conjugated Microporous Polymers via Solvent-Free Ionothermal Cyclotrimerization of Methyl Ketones. *Chem. Mater.* **2021,** *33* (21), 8334-8342.
27. Liu, M.; Guo, L.; Jin, S.; Tan, B., Covalent triazine frameworks: synthesis and applications. *J. Mat. Chem. A* **2019,** *7* (10), 5153-5172.
28. Maschita, J.; Banerjee, T.; Savasci, G.; Haase, F.; Ochsenfeld, C.; Lotsch, B. V., Ionothermal Synthesis of Imide-Linked Covalent Organic Frameworks. *Angew. Chem. Int. Ed.* **2020,** *59* (36), 15750-15758.
29. Krishnaraj, C.; Jena, H. S.; Leus, K.; Van Der Voort, P., Covalent triazine frameworks – a sustainable perspective. *Green Chem.* **2020,** *22* (4), 1038-1071.
30. Rieth, A. J.; Wright, A. M.; Skorupskii, G.; Mancuso, J. L.; Hendon, C. H.; Dincă, M., Record-Setting Sorbents for Reversible Water Uptake by Systematic Anion Exchanges in Metal–Organic Frameworks. *J. Am. Chem. Soc.* **2019,** *141* (35), 13858-13866.
31. Jaramillo, D. E.; Jiang, H. Z. H.; Evans, H. A.; Chakraborty, R.; Furukawa, H.; Brown, C. M.; Head-Gordon, M.; Long, J. R., Ambient-Temperature Hydrogen Storage via Vanadium(II)-Dihydrogen Complexation in a Metal–Organic Framework. *J. Am. Chem. Soc.* **2021,** *143* (16), 6248-6256.
32. Stubbs, A. W.; Dincă, M., Selective Oxidation of C–H Bonds through a Manganese(III) Hydroperoxo in MnII-Exchanged CFA-1. *Inorg. Chem.* **2019,** *58* (19), 13221-13228.
33. Bagi, S.; Wright, A. M.; Oppenheim, J.; Dincă, M.; Román-Leshkov, Y., Accelerated Synthesis of a Ni_2Cl_2(BTDD) Metal–Organic Framework in a Continuous Flow Reactor for Atmospheric Water Capture. *ACS Sustain. Chem. Eng.***2021,** *9* (11), 3996-4003.
34. Wang, Y.; Huang, N.-Y.; Shen, J.-Q.; Liao, P.-Q.; Chen, X.-M.; Zhang, J.-P., Hydroxide Ligands Cooperate with Catalytic Centers in Metal–Organic Frameworks for Efficient Photocatalytic CO_2 Reduction. *J. Am. Chem. Soc.* **2018,** *140* (1), 38-41.
35. Tulchinsky, Y.; Hendon, C. H.; Lomachenko, K. A.; Borfecchia, E.; Melot, B. C.; Hudson, M. R.; Tarver, J. D.; Korzyński, M. D.; Stubbs, A. W.; Kagan, J. J.; Lamberti, C.; Brown, C. M.; Dincă, M., Reversible Capture and Release of Cl_2 and Br_2 with a Redox-Active Metal–Organic Framework. *J. Am. Chem. Soc.* **2017,** *139* (16), 5992-5997.
36. Wang, K.; Yang, L.-M.; Wang, X.; Guo, L.; Cheng, G.; Zhang, C.; Jin, S.; Tan, B.; Cooper, A., Covalent Triazine Frameworks via a Low-Temperature Polycondensation Approach. *Angew. Chem. Int. Ed.* **2017,** *56* (45), 14149-14153.
37. Lee, J.-S. M.; Briggs, M. E.; Hasell, T.; Cooper, A. I., Hyperporous Carbons from Hypercrosslinked Polymers. *Adv. Mater.* **2016,** *28* (44), 9804-9810.
38. Denysenko, D.; Grzywa, M.; Tonigold, M.; Streppel, B.; Krkljus, I.; Hirscher, M.; Mugnaioli, E.; Kolb, U.; Hanss, J.; Volkmer, D., Elucidating Gating Effects for Hydrogen Sorption in MFU-4-Type Triazolate-Based Metal–Organic Frameworks Featuring Different Pore Sizes. *Chem. Eur. J.* **2011,** *17* (6), 1837-1848.
39. Galli, S.; Masciocchi, N.; Colombo, V.; Maspero, A.; Palmisano, G.; López-Garzón, F. J.; Domingo-García, M.; Fernández-Morales, I.; Barea, E.; Navarro, J. A. R., Adsorption of Harmful Organic Vapors by Flexible Hydrophobic Bis-pyrazolate Based MOFs. *Chem. Mater.* **2010,** *22* (5), 1664-1672.
40. Rosi, N. L.; Kim, J.; Eddaoudi, M.; Chen, B.; O'Keeffe, M.; Yaghi, O. M., Rod Packings and Metal−Organic Frameworks Constructed from Rod-Shaped Secondary Building Units. *J. Am. Chem. Soc.* **2005,** *127* (5), 1504-1518.
41. Kapelewski, M. T.; Geier, S. J.; Hudson, M. R.; Stück, D.; Mason, J. A.; Nelson, J. N.; Xiao, D. J.; Hulvey, Z.; Gilmour, E.; FitzGerald, S. A.; Head-Gordon, M.; Brown, C. M.; Long, J. R., M_2(*m*-dobdc) (M = Mg, Mn, Fe, Co, Ni) Metal–Organic Frameworks Exhibiting Increased Charge Density and Enhanced H_2 Binding at the Open Metal Sites. *J. Am. Chem. Soc.* **2014,** *136* (34), 12119-12129.
42. Röß-Ohlenroth, R.; Bredenkötter, B.; Volkmer, D., Organometallic MFU-4l(arge) Metal–Organic Frameworks. *Organometallics* **2019,** *38* (18), 3444-3452.
43. Lee, J.-S. M.; Briggs, M. E.; Hu, C.-C.; Cooper, A. I., Controlling electric double-layer capacitance and pseudocapacitance in heteroatom-doped carbons derived from hypercrosslinked microporous polymers. *Nano Energy* **2018,** *46*, 277-289.
44. Hu, C.; Xiao, Y.; Zhao, Y.; Chen, N.; Zhang, Z.; Cao, M.; Qu, L., Highly nitrogen-doped carbon capsules: scalable preparation and high-performance applications in fuel cells and lithium ion batteries. *Nanoscale* **2013,** *5* (7), 2726-2733.
45. *ASM Handbook Volume 2: Properties and Selection: Nonferrous Alloys and Special-Purpose Materials*. ASM International: 1990; Vol. 2, p 1328.

46. Denysenko, D.; Jelic, J.; Reuter, K.; Volkmer, D., Postsynthetic Metal and Ligand Exchange in MFU-4l: A Screening Approach toward Functional Metal–Organic Frameworks Comprising Single-Site Active Centers. *Chem. Eur. J.* **2015,** *21* (22), 8188-8199.
47. Lu, Y.; Tonigold, M.; Bredenkötter, B.; Volkmer, D.; Hitzbleck, J.; Langstein, G., A Cobalt(II)-containing Metal-Organic Framework Showing Catalytic Activity in Oxidation Reactions. *Z. Anorg. Allg. Chem.* **2008,** *634* (12-13), 2411-2417.
48. Park, S. S.; Tulchinsky, Y.; Dincă, M., Single-Ion Li+, Na+, and Mg2+ Solid Electrolytes Supported by a Mesoporous Anionic Cu–Azolate Metal–Organic Framework. *J. Am. Chem. Soc.* **2017,** *139* (38), 13260-13263.
49. Wang, Z.; Xie, Q.; Wang, Y.; Shu, Y.; Li, C.; Shen, Y., The fixation of CO_2 by epoxides over nickel-pyrazolate-based metal–organic frameworks. *New J. Chem.* **2020,** *44* (42), 18319-18325.
50. Choi, H. J.; Dincă, M.; Long, J. R., Broadly Hysteretic H_2 Adsorption in the Microporous Metal–Organic Framework Co(1,4-benzenedipyrazolate). *J. Am. Chem. Soc.* **2008,** *130* (25), 7848-7850.
51. Choi, H. J.; Dincă, M.; Dailly, A.; Long, J. R., Hydrogen storage in water-stable metal–organic frameworks incorporating 1,3- and 1,4-benzenedipyrazolate. *Energy Environ.l Sci.* **2010,** *3* (1), 117-123.
52. Fang, Z.; Bueken, B.; De Vos, D. E.; Fischer, R. A., Defect-Engineered Metal–Organic Frameworks. *Angew. Chem. Int. Ed.* **2015,** *54* (25), 7234-7254.
53. Gonzalez, M. I.; Kapelewski, M. T.; Bloch, E. D.; Milner, P. J.; Reed, D. A.; Hudson, M. R.; Mason, J. A.; Barin, G.; Brown, C. M.; Long, J. R., Separation of Xylene Isomers through Multiple Metal Site Interactions in Metal–Organic Frameworks. *J. Am. Chem. Soc.* **2018,** *140* (9), 3412-3422.
54. Kapelewski, M. T.; Runčevski, T.; Tarver, J. D.; Jiang, H. Z. H.; Hurst, K. E.; Parilla, P. A.; Ayala, A.; Gennett, T.; FitzGerald, S. A.; Brown, C. M.; Long, J. R., Record High Hydrogen Storage Capacity in the Metal–Organic Framework Ni_2(*m*-dobdc) at Near-Ambient Temperatures. *Chem. Mater.* **2018,** *30* (22), 8179-8189.
55. Gonzalez, M. I.; Mason, J. A.; Bloch, E. D.; Teat, S. J.; Gagnon, K. J.; Morrison, G. Y.; Queen, W. L.; Long, J. R., Structural characterization of framework–gas interactions in the metal–organic framework Co_2(dobdc) by in situ single-crystal X-ray diffraction. *Chem. Sci.* **2017,** *8* (6), 4387-4398.
56. Gygi, D.; Bloch, E. D.; Mason, J. A.; Hudson, M. R.; Gonzalez, M. I.; Siegelman, R. L.; Darwish, T. A.; Queen, W. L.; Brown, C. M.; Long, J. R., Hydrogen Storage in the Expanded Pore Metal–Organic Frameworks M_2(dobpdc) (M = Mg, Mn, Fe, Co, Ni, Zn). *Chem. Mater.* **2016,** *28* (4), 1128-1138.
57. Díaz-García, M.; Sánchez-Sánchez, M., Synthesis and characterization of a new Cd-based metal-organic framework isostructural with MOF-74/CPO-27 materials. *Microporous Mesoporous Mater.* **2014,** *190*, 248-254.
58. Borycz, J.; Paier, J.; Verma, P.; Darago, L. E.; Xiao, D. J.; Truhlar, D. G.; Long, J. R.; Gagliardi, L., Structural and Electronic Effects on the Properties of Fe_2(dobdc) upon Oxidation with N_2O. *Inorg. Chem.* **2016,** *55* (10), 4924-4934.
59. Xiao, D. J.; Bloch, E. D.; Mason, J. A.; Queen, W. L.; Hudson, M. R.; Planas, N.; Borycz, J.; Dzubak, A. L.; Verma, P.; Lee, K.; Bonino, F.; Crocellà, V.; Yano, J.; Bordiga, S.; Truhlar, D. G.; Gagliardi, L.; Brown, C. M.; Long, J. R., Oxidation of ethane to ethanol by N2O in a metal–organic framework with coordinatively unsaturated iron(II) sites. *Nat. Chem.* **2014,** *6* (7), 590-595.
60. Bloch, E. D.; Murray, L. J.; Queen, W. L.; Chavan, S.; Maximoff, S. N.; Bigi, J. P.; Krishna, R.; Peterson, V. K.; Grandjean, F.; Long, G. J.; Smit, B.; Bordiga, S.; Brown, C. M.; Long, J. R., Selective Binding of O_2 over N_2 in a Redox–Active Metal–Organic Framework with Open Iron(II) Coordination Sites. *J. Am. Chem. Soc.* **2011,** *133* (37), 14814-14822.
61. Queen, W. L.; Bloch, E. D.; Brown, C. M.; Hudson, M. R.; Mason, J. A.; Murray, L. J.; Ramirez-Cuesta, A. J.; Peterson, V. K.; Long, J. R., Hydrogen adsorption in the metal–organic frameworks Fe_2(dobdc) and $Fe_2(O_2)$(dobdc). *Dalton Trans.* **2012,** *41* (14), 4180-4187.
62. Bloch, E. D.; Queen, W. L.; Chavan, S.; Wheatley, P. S.; Zadrozny, J. M.; Morris, R.; Brown, C. M.; Lamberti, C.; Bordiga, S.; Long, J. R., Gradual Release of Strongly Bound Nitric Oxide from $Fe_2(NO)_2$(dobdc). *J. Am. Chem. Soc.* **2015,** *137* (10), 3466-3469.
63. Pu, S.; Wang, J.; Li, L.; Zhang, Z.; Bao, Z.; Yang, Q.; Yang, Y.; Xing, H.; Ren, Q., Performance Comparison of Metal–Organic Framework Extrudates and Commercial Zeolite for Ethylene/Ethane Separation. *Ind. Eng. Chem. Res.* **2018,** *57*.
64. Cho, H.-Y.; Yang, D.-A.; Kim, J.; Jeong, S.-Y.; Ahn, W.-S., CO2 adsorption and catalytic application of Co-MOF-74 synthesized by microwave heating. *Catalysis Today* **2012,** *185* (1), 35-40.
65. Bloch Eric, D.; Queen Wendy, L.; Krishna, R.; Zadrozny Joseph, M.; Brown Craig, M.; Long Jeffrey, R., Hydrocarbon Separations in a Metal-Organic Framework with Open Iron(II) Coordination Sites. *Science* **2012,** *335* (6076), 1606-1610.
66. Xiao, D. J.; Oktawiec, J.; Milner, P. J.; Long, J. R., Pore Environment Effects on Catalytic Cyclohexane Oxidation in Expanded Fe_2(dobdc) Analogues. *J. Am. Chem. Soc.* **2016,** *138* (43), 14371-14379.
67. Reed, D. A.; Keitz, B. K.; Oktawiec, J.; Mason, J. A.; Runčevski, T.; Xiao, D. J.; Darago, L. E.; Crocellà, V.; Bordiga, S.; Long, J. R., A spin transition mechanism for cooperative adsorption in metal–organic frameworks. *Nature* **2017,** *550* (7674), 96-100.
68. Lefebvre, J.; Galli, F.; Bianchi, C. L.; Patience, G. S.; Boffito, D. C., Experimental methods in chemical engineering: X-ray photoelectron spectroscopy-XPS. *Can. J. Chem. Eng.* **2019,** *97* (10), 2588-2593.
69. Sun, L.; Hendon, C. H.; Minier, M. A.; Walsh, A.; Dincă, M., Million-Fold Electrical Conductivity Enhancement in Fe_2(DEBDC) versus Mn_2(DEBDC) (E = S, O). *J. Am. Chem. Soc.* **2015,** *137* (19), 6164-6167.
70. Sun, L.; Hendon, C. H.; Park, S. S.; Tulchinsky, Y.; Wan, R.; Wang, F.; Walsh, A.; Dincă, M., Is iron unique in promoting electrical conductivity in MOFs? *Chem. Sci.* **2017,** *8* (6), 4450-4457.

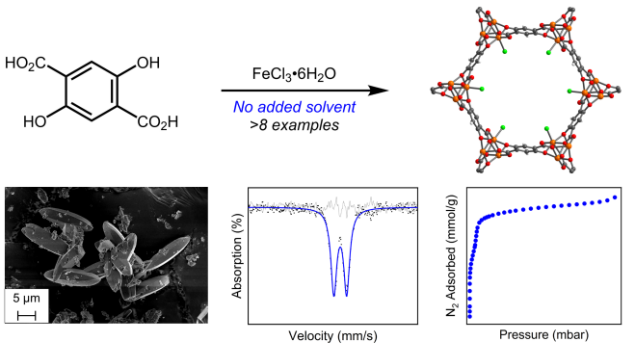

Highly Crystalline & Porous Metal-Organic Frameworks Prepared Without Solvent